 FDMP, vol.6, no.4, pp.399-408, 2010

Droplet Behavior within an LPP Ambiance

M. Chrigui[1,2], L. Schneider[1], A. Zghal[2], A. Sadiki[1] and J. Janicka[1]

Abstract: This paper deals with the numerical simulation of droplet dispersion and evaporation within an LPP (Lean Premix Prevaporized) burner. The Eulerian-Lagrangian approach was used for this purpose, and a fully two way-coupling was accounted for. For the phase transition, a non-equilibrium evaporation model was applied that differs strongly from the equilibrium one where there are high evaporation rates. The non-equilibrium conditions were fulfilled in the investigated configuration, as the droplets at the inlet had a mean diameter of 50 μm. The numerical results of water droplet velocities, corresponding fluctuations, and diameters were compared with experimental data. Good agreement was found.

Keywords: Euler-Lagrange, dispersion, evaporation, two-way coupling.

1 Introduction

Efficiency and emissions are mainly determined by the manner in which the oxidizer and gaseous fuel are prepared. Several researchers have studied the problems of spray dispersion, evaporation and combustion experimentally and numerically. Oefelein and Aggarwal (2000) tried to show the differences between classical low-pressure and high-pressure evaporation models. They found that the high-pressure drop regression process is different from that in the preceding subcritical low-pressure state. Miller et al. (1998) performed an evaluation of existing evaporation models that can be used to describe droplets of various diameters at low pressure. They realized that non-equilibrium effects become significant when the initial droplet diameter is less than 50 μm. Of particular interest is the vaporization of small single-component water, benzene, decane, heptane and hexane droplets in high temperature environments. These types of droplets can be found in many spray mixing and spray combustion processes. Other liquids, like paints, liquid catalyzers, suspensions and emulsions, are used in the material processing industry

[1] Institute for Energy and Powerplant Technology, Department of Mechanical Engineering, Technische Universität Darmstadt, Germany

[2] Laboratory of Mechanics, Solids, Structures and Technological Development, ESSTT, Tunisia

to generate functional or reactive surfaces, control the temperature of heated semi-finished steel products or produce granulates or powders in the food and pharmaceutical industry (cf. Blei (2006)). In all these processes, the evaporation is the controlling phenomenon. Spray combustion is also of relevance to the material processing industry. In large sintering processes, for example, the combustion of heavy oil is the source of the sintering energy.

Evaporation effects, fully two-way coupling, and other related inter-phase transport modifications used for turbulence and vaporization in RANS (Reynolds-averaged Navier-Stokes equations) and Large Eddy Simulation (LES) are not complete nor physically sufficient in numerical simulations. However, RANS-based calculations are state of the art in many engineering design applications because of their economical computation costs. Turbulent reactive spray processes are lacking due to the complexity of the problem. Réveillon and Vervisch (1998) applied a three dimensional Direct Numerical Simulation (DNS) to simulate the spray vaporization and combustion. The simulations, however, were confined to clusters of a limited number of droplets due to high computational costs. Mashayek (1999) investigated evaporating and reacting fuel droplets in forced turbulent flows. He realized that the combustion process is significantly affected by the rate of evaporation. Pursuant to this, the investigations reported here aim to investigate droplet behavior, e.g. entrainment, dispersion and evaporation, within the carrier phase. The inlet conditions correspond to those of the partially premixed gas turbine.

2 Implemented models

2.1 Modeling

The turbulent fluid phase is described in a RANS modeling approach. The transport equations were solved for the mass conservation, velocity components (u, v, w), enthalpy, turbulent kinetic energy and turbulent dissipation rate (for example, Réveillon and Vervisch (1998)). The transport equations were modified for two-phase flow description by including source terms for phase exchange and phase transition processes (Sadiki et al., 2005). Models accounting for the induced turbulence attenuation or augmentation were applied for two-way coupling (Lain and Sommerfeld (2003)).

Evaporation is commonly modeled using mass transfer terms that are incorporated into the mass balance equations for gas and droplets. The models for this transfer term are derived from an equilibrium configuration in which an evaporating droplet is suspended in a non-moving gas environment (cf. Abramson and Sirignano (1989)). A characteristic parameter (Eq. 1) was introduced to characterize the deviation of phase transition on the droplet surface from equilibrium.

It depends, among other things, on the ratio of the non-equilibrium and quasi-equilibrium Peclet numbers. For a detailed analysis and a comparative evaluation of these models, see Miller et al. (1998) and its references. For the equilibrium models, the molar mass fraction χ_s is related to the saturation pressure through the Clausius-Clapeyron equation (Abramson and Sirignano (1989). The following relation determines the molar mass fraction χ_s in a non-equilibrium evaporation model:

$$\chi_{s,neq} = \chi_{s,eq} - \left(\frac{L_K}{d/2}\right)\beta_L, \tag{1}$$

where $\beta_L = -\left(\frac{3\,\mathrm{Pr}_G\,\tau_d}{2}\right)\frac{\dot{m}}{m}$ represents half of the blowing Peclet number. d is the droplet diameter, Pr_G is the Prandtl number, L_K represents the Knudsen length and τ_d is the particle relaxation time.

Abramson and Sirignano (1989) introduced modified Nusselt and Sherwood numbers to represent Stefan's flow and its effect on heat and mass transfer.

A dispersion model is needed to obtain the velocity fluctuations of the gas phase at the position of the droplets, which are required for the computation of the droplet equation of motion. The Markov Sequence Model based on the calculation of Lagrangian and Eulerian correlations was used (Chrigui et al. (2004).

2.2 Numerical Issues

A three-dimensional CFD code was used, in which the equations for the gas phase are solved by finite volume method. The diffusion terms were discretized using flux blending schemes on a non-orthogonal, block-structured grid. The velocity pressure coupling was accomplished using a SIMPLE algorithm. The whole system was solved using the SIP solver. The Lagrangian equations for droplets were discretized using a first order scheme and solved explicitly. The source terms for the gas phase were computed in each cell using contributions from all relevant droplets.

The interaction between the continuous and dispersed phases consists of couplings between two codes. After the convergence of the gas phase, the gas variables are kept frozen and all the droplets representing the entire spray are injected into the computational domain. Due to the presence of the droplets' source terms, the conventional residuals are characterized by a jump after each coupling. To avoid oscillations, an additional under-relaxation technique should also be employed for droplet source terms.

The droplet injection is based on a stochastic approach by considering the droplet mass flux and the droplet size distributions obtained from the experimental measurements at the inlet, near the nozzle exit.

3 Configuration description

The Partially Pre-vaporized Spray Burner (PPSB) presented by Baessler at al. (2006) was used to study the evaporation and combustion of kerosene (water was also studied but only for evaporation). This burner consists of an ultrasonic nozzle, a heating coil to control the temperature of the gas flow, a mixing tube, a hot wire and a water-cooled ring, and a combustion tube (Figure 1, right). The main part of the air (300 l_n/min)[1] enters the configuration through the heating coils where it can reach temperatures of up to 418 K. 15 ml/min kerosene fuel (or water) and 20 l_n/min air (at 293 K) are fed into the ultrasonic nozzle. The heated air is further accelerated and mixed with the spray in the mixing tube. The length of the mixing tube, L (Figure 1, right), is between 0.5 and 1.0 m.

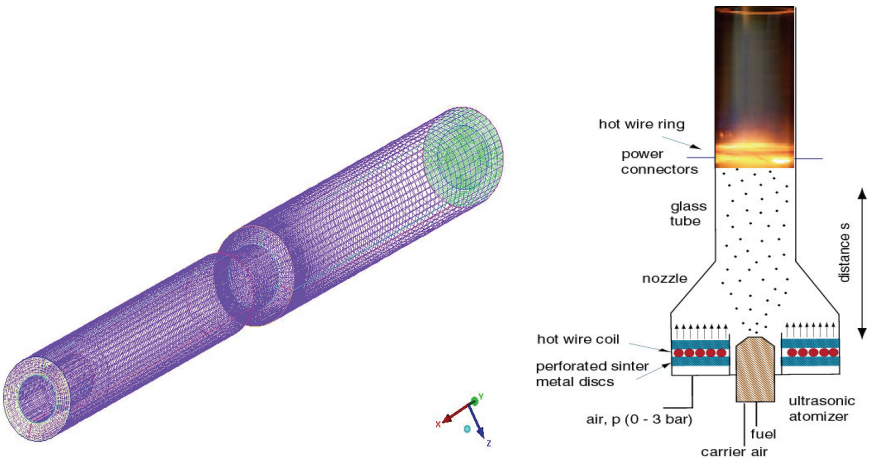

Figure 1: Partially Pre-vaporized Spray Burner (PPSB). Left: grid. Right: experiment. From Baessler at al. (2006)

Downstream of the mixing zone, a contraction (Figure 1, left) adjusts the flow velocity to prevent flame flashback. Above this contraction, the hot wire ring is used to ignite the mixture. The water-cooled ring is used to stabilize the flame. Downstream of the contraction, the flame is confined in a glass tube of diameter 90 mm. Baessler and co. used Phase Doppler Anemomentry to carry out measurements (Baessler at al. (2006) and Baessler (2008). The experimental results used later in this work are taken from the same references.

[1] *normal liter/minute*, gas flow at 0°C and 1.013 bar.

The overall mesh for the single annular combustor is about 340,000 control volumes (Figure 1, left). The grid has 18 multi-connected domains, i.e. they consist of several separate flow-paths that interact with each other. Cartesian coordinates and hexahedral cells were used to generate the mesh. The boundaries, given at inlets, include specification of the gas phase and the droplet velocity components, the droplet mass flow, the diameter distributions and the temperature. The inlet conditions for the turbulent kinetic energy are calculated using a turbulence intensity of 10% of the resultant velocity through an inlet. The distribution of the dissipation rate is estimated using the expression

$$\varepsilon = C_{\mu}^{3/4} \frac{k^{3/2}}{0.41 \cdot \Delta r}. \tag{2}$$

Here, the turbulent length scale was assumed to be equal to the diameter of the hole or opening of the inlet.

4 Results and discussion

The water droplets (15 *ml/min*) used in the frame of this configuration have a Sauter Mean Diameter (SMD) of $53\mu m$ with a small Stokes number. For this reason, the droplets are able to easily follow the carrier phase. The first qualitative results of the dispersed phase, i.e. mean velocity and the corresponding fluctuation of the droplets, are presented in Figure 2. Due to the contraction at the end of the pre-evaporation zone, the axial velocity increased up to 2.4 m/s. This increase in the droplet velocity follows the acceleration of the gas flow. This is intended to prevent flashback of the flame into the mixing tube.

The RMS values of the velocity in radial direction and the droplet mean diameter are plotted in Figure 3 for the test case with heated main airflow of 363 K. A large number of droplets are able to cross the mixing tube. The highest droplet radial velocity fluctuations are observed at the sudden expansion, namely in the shear flow regions, due to the jet formed by the geometry contraction. The length of the mixing tube, L, is 80 cm.

Figure 4 shows a comparison between experimental and numerical results for the mean axial velocity and RMS values of the droplets as a function of the radius. These results are taken at distance *s= 81 cm* (Figure 1, right) from the fuel nozzle outlet in different radial and tangential directions. There is good agreement between the two for the mean velocity. The fact that the velocity varies at a fixed distance *s* may be due to the anisotropic nature of the dispersed phase flow. However, due to the complexity of the process and rather poor statistics for the droplet diameter, it is difficult to draw strong conclusion from these results. The numerical

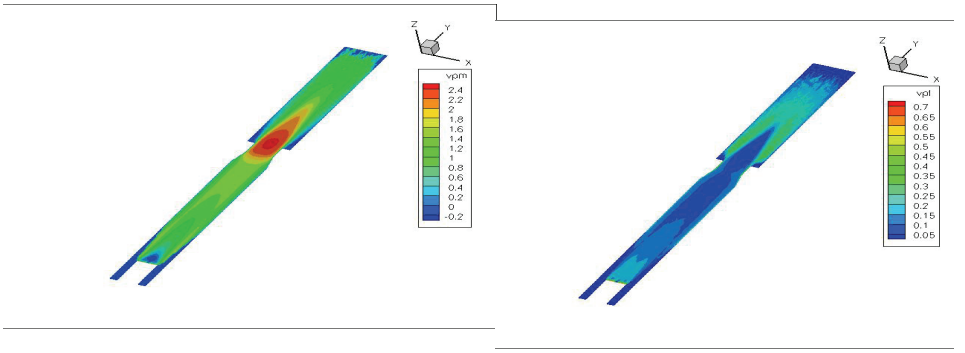

Figure 2: Water droplet mean velocity [m/s] (left) and corresponding fluctuation [m/s] (right). Test case with heated air at 363 K.

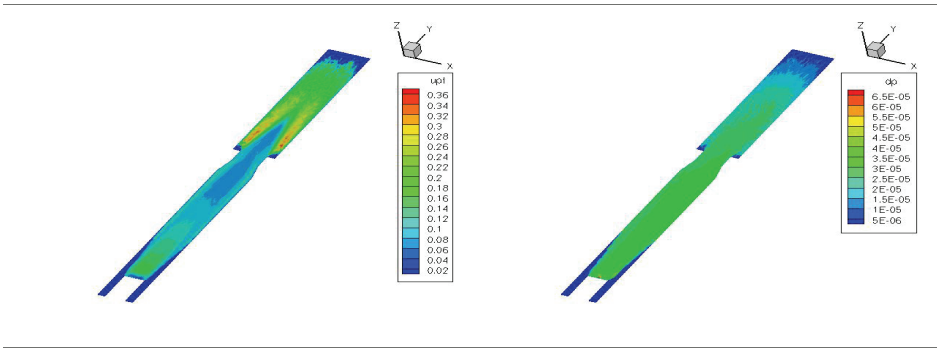

Figure 3: RMS values of the droplet velocity in radial direction [m/s] (left), mean diameter [m] (right) in the test case of water and heated air at 363 K.

results for the axial velocity fluctuation are under-estimated. This is most likely due to the droplet dispersion model or to an under-prediction of the turbulent kinetic energy of the carrier phase. No experimental data is available for the latter, so it cannot be compared to numerical simulations.

For the test case with preheated air (363 K), the comparison between experiment and numerical measurement of the mean velocity and its fluctuations is presented in Figure 5. Once again, there are plausible results for the amplitude of the axial velocity but an under-estimation of the fluctuations. The numerical simulations predict an almost constant value for the mean axial velocity of the droplets at a fixed radius, i.e. there is little dependency on radial or tangential direction.

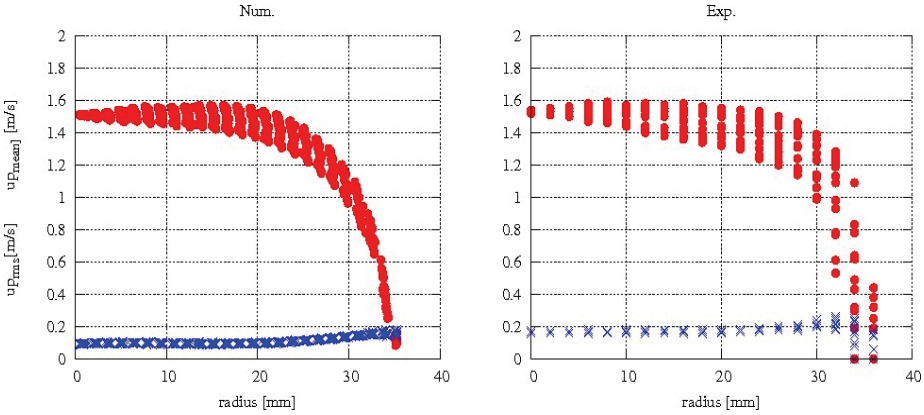

Figure 4: Comparison between numerical (left) and experimental (right) measurements of the mean velocity (dots) and its fluctuations (crosses) at a distance of 81 cm from the inlet for the test case with main airflow at 293 K.

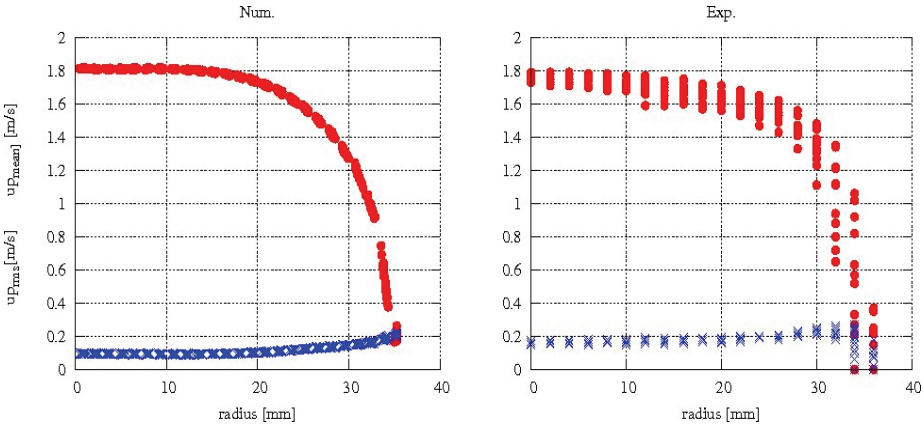

Figure 5: Comparison between numerical (left) and experimental (right) results for the mean droplet velocity (dots) and its fluctuations (crosses) at a distance of 81 cm from the inlet for the test case of main airflow at 363 K.

Among other things, the droplet evaporation rate was checked by the distribution of the droplet diameters. Figure 6 and Figure 7 show comparisons between numerical and experimental measurements of the different diameter distributions at two distances, *s=61 cm* and *s=81 cm*, from the fuel nozzle outlet with temperatures 293 K and 363 K of the main air at the inlet. The results are plotted for radial and tangential positions, and for a constant distance, s. The boundary conditions play a major

role in the distribution of the droplet diameters, i.e. locations, probability density function of all classes and corresponding velocities, which were only provided approximately due to difficulty in the measurement techniques. Nevertheless, there was very good agreement in the main airflow observed in the 293 K case. For the case with preheated air (363 K), there was good agreement until the distance of *s=61cm*. Downstream of this position, the numerical simulations predict a faster evaporation rate than the experimental measurements. This small disagreement is observed only for the Sauter mean diameter dp_{32}.

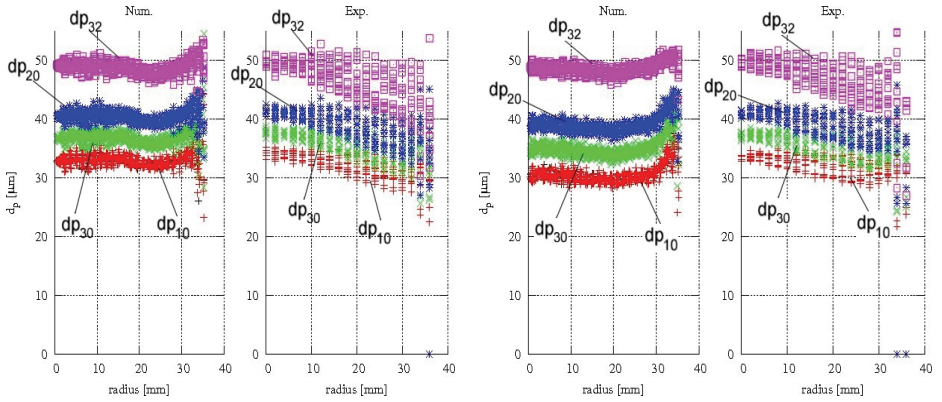

Figure 6: Comparison between numerical and experimental results for the arithmetic mean diameter dp_{10}, surface area mean diameter dp_{20}, volume mean diameter dp_{30} and the Sauter mean diameter dp_{32} at 61 cm (left diagram) and 81 cm (right diagram) from the nozzle. The main air temperature is 293 K.

5 Conclusion

Spray and flow simulations of water droplets evaporating in a convective gas flow environment were performed. These conditions are found in industrial applications, such as the LPP concept in gas turbines. The numerically predicted vaporization characteristics were compared to experimental measurements and showed very good agreement, i.e. the models used for the description of the dispersed phase were able to describe not only the phase transition process but also the interaction with other phenomena, such as turbulence and dispersion. The accurate prediction of the droplet diameters demonstrates that the evaporation degree at the end of the prevaporization length was well captured within non-equilibrium multiphase flow conditions. The discrepancies, seen in the droplet velocity fluctuations, could be

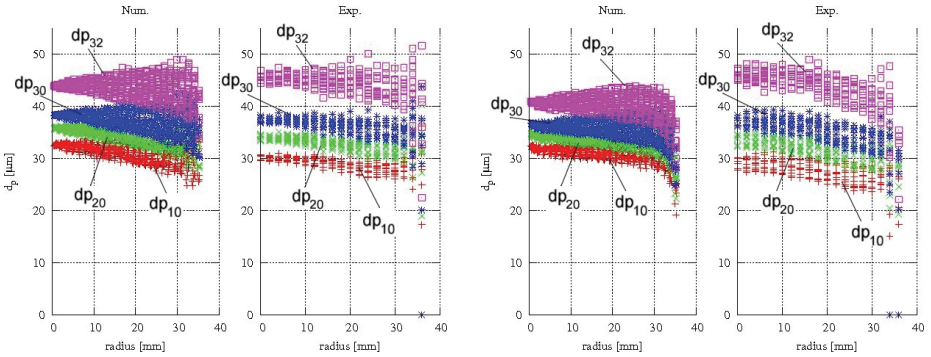

Figure 7: Comparison between numerical and experimental results for the arithmetic mean diameter dp_{10}, surface area mean diameter dp_{20}, volume mean diameter dp_{30}, and the Sauter mean diameter dp_{32} at 61 cm (left diagram) and 81 cm (right diagram) from the nozzle. The main air temperature is 363 K.

reduced by considering the drift correction term as it accounts for the stress gradients which are responsible for enhancing the pressure gradient, as in Sommerfeld et al. (1993). The last two points mentioned have an important effect on fuel oxidizer preparation, which is the aim of this research project. Further results that account for combustion processes, e.g. considering kerosene droplets, are being analyzed and compared with experimental data (Baessler at al. (2006) and Baessler (2008)) and will be published in the near future.

Acknowledgement: We gratefully acknowledge the ESA (European Space Agency) for their financial support.

References

Abramson B., Sirignano W.A. (1989): Droplet Vaporization Model for Spray Combustion Calculations, *Int. J. Heat Mass Transfer*, Vol. 32, pp. 1605-1618.

Baessler S. (2008): *Einfluss des Vorverdampfungsgrades auf die Stickoxidbildung in Sprayflammen*, Dissertation, Technical University Munich (German).

Baessler S., Moesl K., Sattelmayer T. (2006): Nox emissions of a premixed partially vaporized kerosene spray flame, *Proceedings of ASME Turbo Expo Power for Land, Sea, and Air*, Barcelona, Catalonia, Spain.

Blei S. (2006): On the interaction of non-uniform particles during the spray drying process. Experiments and Modelling with the Euler-Lagrange Approach, *Dissertation,* Universität Halle-Wittenberg.

Chrigui M., Ahmadi G., Sadiki A. (2004): Study on Interaction in Spray between Evaporating Droplets and Turbulence Using Second Order Turbulence RANS Models and a Lagrangian Approach, *Progress in Computational Fluid Dynamics*, Vol. 4, pp. 162-174.

Lain S., Sommerfeld M. (2003): Turbulence modulation in dispersed two-phase flow laden with solids from a Lagrangian perspective, *Int. J. Heat and Fluid Flow,* Vol. 24, pp. 616-625.

Mashayek F. (1999): Simulations of reacting droplets dispersed in isotropic turbulence, *AIAA J.*, Vol. 37, pp. 1420-1425.

Miller R.S., Harstad K., Bellan J. (1998): Evaluation of equilibrium and non-equilibrium evaporation models for droplet gas liquid flow simulation, *Int. J. Multiphase Flow*, Vol. 24, pp. 1025-1055.

Oefelein J.C., Aggarwal S.K. (2000): Toward a unified high pressure drop model for spray simulation, *Center for Turbulence Research,* Proceedings of Summer Program.

Reveillon J., Vervisch L. (1998): Accounting for spray vaporization in turbulent combustion modeling, *Center for Turbulence Research,* Proceedings of the Summer Program.

Sadiki A., Chrigui M., Janicka J., Maneshkarimi M.R. (2005): Modeling and simulation of effects of turbulence on vaporization, mixing and combustion of liquid fuel sprays, *Flow, Turbulence and Combustion,* Vol. 75, pp. 105-130.

Sommerfeld, M., Kohnen, G., Rüger, M. (1993): Some open questions and inconsistencies of Lagrangian particle dispersion models, *Proc. Ninth Symp. on Turbulent Shear Flow, Tokyo, Japan.*